Block-Spreading Codes for Impulse Radio Multiple Access through ISI channels

Liuqing Yang and Georgios B. Giannakis
Dept. of ECE
Univ. of Minnesota
200 Union Street SE
Minneapolis, MN 55455

Abstract— **Transmitting digital information using ultra-short pulses, Impulse Radio (IR) has received increasing interest for Multiple Access (MA). Analog IRMA utilizes pulse-position modulation (PPM) and random time-hopping codes to mitigate inter-symbol interference (ISI) and suppress multiuser interference (MUI) statistically. We develop an all-digital IRMA scheme that relies on block-spreading and judiciously designed transceiver pairs to eliminate MUI deterministically, and regardless of ISI multipath effects.**

I. INTRODUCTION

Impulse radio is an ultra-wide band communication system with attractive features for baseband multiple access, tactical wireless communications, and multimedia services. An IR transmission consists of a pseudo-randomly shifted train of very short pulses, where the information is encoded in the shift via pulse position modulation (PPM). The random shifts combined with the short pulse shaper, and the data modulation result in a transmitted signal with low power spectral density spread across the ultra-wide bandwidth.

IR equipped with time-hopping codes has been applied to multiuser communications in [6], where it is referred to as impulse radio multiple access (IRMA). Subsequent works have focused on optimizing the efficiency of IRMA by characterizing the channel, improving the modulation format, and addressing networking aspects; see [1, 2, 8, 9, 10] and references therein.

In analog IRMA schemes proposed so far, the MUI is randomized, and only statistically suppressed, provided that (strict) power control is successfully applied. A digital IRMA model was developed in [4]. This scheme is tailored to a *downlink* scenario, and relies on multiuser detection (MUD), which brings benefits over the statistical MUI cancellation when the number of users is small, and thus the Gaussian approximation of the MUI is no longer valid. However, [4] is not applicable to uplink scenario; but even in the downlink, the receiver designs require inversion of very large size matrices.

In this paper, we develop an all-digital Impulse Radio that relies on block-spreading to gain resilience to MUI and ISI. By parsing the transmitted information stream into blocks and applying block-spreading, and chip-interleaving before transmission, MUI can be eliminated *deterministically* at the receiver. As a result, our scheme renders the *multiple access channel equivalent to a set of independent parallel single-user frequency-selective channels with AWGN*, and *any* single-user equalizer can be employed afterwards. The resulting so-called Chip-Interleaved Block-Spread (CIBS) IRMA transceivers have low-complexity, and are applicable to both *uplink* and *downlink* scenarios.

In Section II, we start from a brief review of the continuous-time PPM-IRMA model as described in [4]. Based on this model, the analog and digital equivalent CIBS-IRMA schemes are derived in Section III. Our digital transceiver designs developed in Section IV are based on a specific block-spreading operation, which can be viewed as (and is implemented by) symbol-spreading followed by chip interleaving [12]. Thanks to chip-interleaving and zero padding at the transmitter, mutual orthogonality between different users' codes is preserved even after multipath propagation, which enables deterministic multiuser separation. Consequently, MUD is successfully converted to a set of equivalent single user equalization problems. Simulations are performed in Section V, where comparisons with [4] are shown.

Notation: Bold upper (lower) letters denote matrices (column vectors); $(\cdot)^T$ and $(\cdot)^{\mathcal{H}}$ denote transpose and Hermitian transpose, respectively; $\delta(\cdot)$ and $\otimes$ stand for Kronecker's delta and Kronecker product, respectively. $\mathrm{E}\{\cdot\}$ for expectation, $\lceil\cdot\rceil$ for integer ceiling; $\mathbf{I}_K$ denotes the identity matrix of size K; $\mathbf{0}_{M\times N}$ denotes an all-zero matrix with size $M \times N$.

II. CONTINUOUS-TIME PPM-IRMA MODELING

To facilitate the transition from the original continuous-time PPM to our block-spreading model, we first briefly review the PPM-IRMA model of [4] in the single-user case.

In PPM-IRMA, for each, e.g., the m-th, user, every transmitted information symbol $s_m(n)$ drawn from the alphabet $\{0, 1, \ldots, A-1\}$ is repeated over N_f frames each having duration T_f. We denote the m-th users' symbol transmitted during the k-th frame as $s_m(\lfloor k/N_f \rfloor)$.

Each frame comprises N_c chips. With T_c denoting chip duration, we have $T_f = N_c T_c + T_g$, where T_g is a guard time introduced to account for processing delay at the receiver between two successively received frames. The m-th user's transmitted waveform is given by:

$$v_m(t) = \sum_{k=-\infty}^{+\infty} w\left(t - kT_f - \tilde{c}_m(k)T_c - \tau_{s_m(\lfloor k/N_f \rfloor)}\right), \quad (1)$$

where $w(t)$ denotes the ultra-short monopulse, and $\tilde{c}_m(k) \in [0, N_c - 1]$ is a periodic time-hopping (TH) pseudo-random sequence with period $P_{\tilde{c}} = N_f$. The role of $\tilde{c}_m(k)$ is to enable multiple access, and security in e.g., military communications. Each segment of duration $N_f T_f$ contains N_f copies of a single symbol (one per frame), and the monopulse is time-shifted in each frame according to the symbol value; e.g., it is shifted by τ_a if $s_m(\lfloor k/N_f \rfloor) = a$, for $a \in [0, 1, \ldots, A-1]$. Let T_w denote the monopulse duration. In order to ensure orthogonal modulation, PPM modulation delays τ_m must satisfy $\tau_a - \tau_{a-1} \geq T_w$, $\forall a \in [1, 2, \ldots, A-1]$. Thus, the chip duration is chosen to satisfy: $T_c \geq AT_w$. One way to model this mapping is to have A parallel branches each realizing a shifted version of the pulse stream. In order to generate the signal, we then only need to

0-7803-7400-2/02/$17.00 © 2002 IEEE

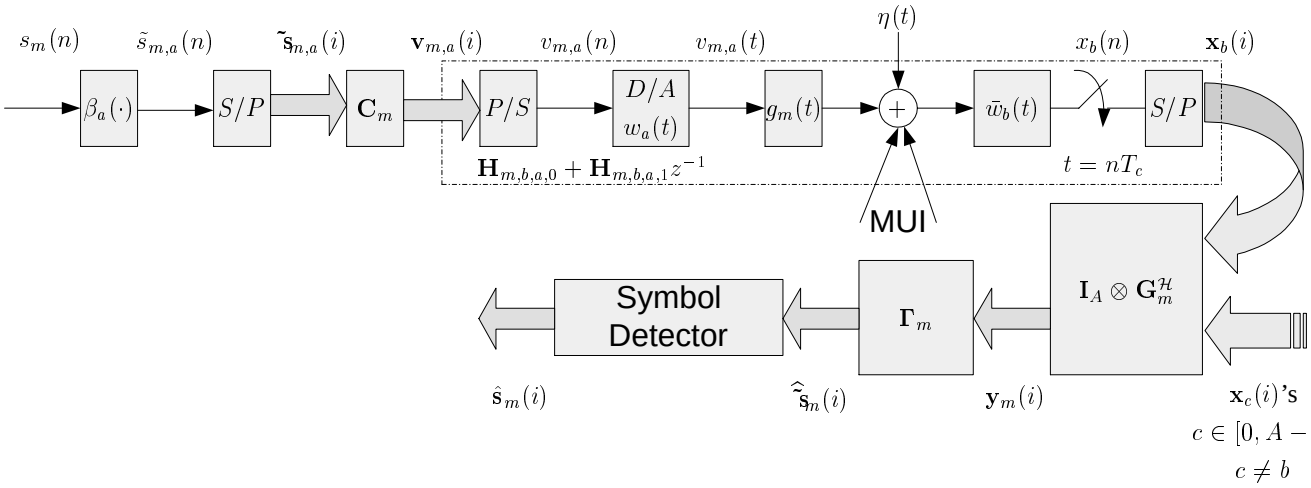

Fig. 1. Continuous and discrete-time equivalent system model of the m-th user (only the a-th branch at the transmitter and the b-th branch at the receiver are shown).

select one branch (out of A) depending on the symbol value. Adopting this viewpoint, we can re-express (1) as:

$$v_m(t) = \sum_{a=0}^{A-1} v_{m,a}(t) \tag{2}$$

with

$$v_{m,a}(t) = \sum_{k=-\infty}^{+\infty} \tilde{s}_{m,a}(k) w\left(t - kT_f - \tilde{c}_m(k)T_c - \tau_a\right), \tag{3}$$

where $\tilde{s}_{m,a}(k) := \beta_a(s_m(\lfloor k/N_f \rfloor))$; and $\beta_a(\cdot)$ captures the branch selection process according to the following definition:

$$\text{for} \qquad s, a \in [0, A-1], \quad \beta_a(s) := \begin{cases} 1 & \text{if } s = a\,, \\ 0 & \text{otherwise.} \end{cases} \tag{4}$$

Upon defining the time-shifted pulses $w_a(t) := w(t - \tau_a)$, and recalling that $T_f = N_c T_c$ for $T_g = 0$, (3) can be rewritten as

$$v_{m,a}(t) = \sum_{k=-\infty}^{+\infty} \tilde{s}_{m,a}(k) w_a\left(t - (kN_c + \tilde{c}_m(k))\,T_c\right). \tag{5}$$

Because $\tilde{c}_m(k) \in [0, N_c - 1]$ is an integer, we infer that $w_a(t)$ in (5) is shifted by an integer multiple of T_c. It is thus possible to view $v_{m,a}(t)$ as a linearly modulated waveform with symbol rate $1/T_c$, and express it as:

$$v_{m,a}(t) = \sum_{n=-\infty}^{+\infty} u_{m,a}(n) w_a(t - nT_c), \tag{6}$$

where $u_{m,a}(n)$ is a sequence that depends on $\tilde{s}_{m,a}(k)$, and $\tilde{c}_m(k)$. Equation (2) can be interpreted as the superposition of A linear modulators each with a different pulse function $w_a(t)$.

Defining the chip-rate code sequence $c_m(n)$ as:

$$c_m(n) := \delta(\lfloor n/N_c \rfloor N_c + \tilde{c}_m(\lfloor n/N_c \rfloor) - n). \tag{7}$$

It can be readily verified by direct substitution that the period of $c_m(n)$ in (7) is $P_c = N_c P_{\tilde{c}}$. The reason we introduced $c_m(n)$ is because the m-th user's chip sequence on the a-th branch $u_{m,a}(n)$ in (6) can be conveniently expressed as:

$$u_{m,a}(n) = \tilde{s}_{m,a}(\lfloor n/N_c \rfloor) c_m(n). \tag{8}$$

From this chip-rate sampled model, the nonlinearly modulated PPM-IRMA model can be viewed as a linearly modulated CDMA system [4].

We have assumed here for simplicity that $T_g = 0$, although the model can encompass $T_g \neq 0$ as well. This can be accomplished by setting $T_g = N_g T_c$ with N_g integer, and restricting the sequence $\tilde{c}_m(k)$ to take its values on $[0, N_c' - 1]$, where $N_c' := N_c - N_g$. Hereafter, we will assume $T_g = 0$.

III. Block IRMA Modeling

The block diagram in Fig. 1 describes a Block-Spreading IRMA model in either *uplink* or *downlink* operation, where only the a-th branch of one user (the m-th user of a maximum of M users) is shown.

Recall that the information carrying stream $\tilde{s}_{m,a}(\lfloor n/N_c \rfloor)$ is constant over the duration of $N_f T_f$ seconds, and is then spread by the user-specific code $c_m(n)$ to generate the chip sequence $u_{m,a}(n)$ in (8). From this perspective, the PPM-IRMA model can be viewed as a CDMA system. Unlike traditional spreading which is performed over a *single symbol*, we here use block spreading that operates on a *block of symbols*. Specifically, the information stream on the a-th branch of the m-th user $\tilde{s}_{m,a}(n)$ is first parsed into blocks of length K:

$$\tilde{\mathbf{s}}_{m,a}(i) := [\tilde{s}_{m,a}(iK), \ldots, \tilde{s}_{m,a}(iK + K - 1)]^T,$$

and then block-spread by a user-specific $P \times K$ spreading matrix $\mathbf{C}_m$ to obtain the $P \times 1$ output vector $\mathbf{u}_{m,a}(i) = \mathbf{C}_m \tilde{\mathbf{s}}_{m,a}(i)$. Viewing each column of $\mathbf{C}_m$ (with the $(k+1)$st column denoted by $\mathbf{c}_{m,k}$) as a separate spreading code for user m, the block spreading operation implements a multi-code transmitter (K codes per user), since we can write the transmitted block as $\mathbf{u}_{m,a}(i) = \sum_{k=0}^{K-1} \tilde{s}_{m,a}(iK + k)\mathbf{c}_{m,k}$ [7].

After Parallel to Serial (P/S) conversion of $\mathbf{u}_{m,a}(i)$, the m-th user's chip sequence on the a-th branch $u_{m,a}(n)$ is pulse shaped to yield the corresponding continuous time signal $v_{m,a}(t) = \sum_{n=-\infty}^{+\infty} u_{m,a}(n) w_a(t - nT_c)$, where T_c is the chip period, and $w_a(t)$ is the chip pulse for symbol a. The transmitted signal $v_{m,a}(t)$ propagates through a channel $g_m(t)$ and is filtered by the receive filter on the b-th branch $\bar{w}_b(t)$, which is matched to $w_b(t)$, where $b \in [0, A-1]$. With $\star$ denoting convolution, let $h_{m,b,a}(l) := (w_a \star g_m \star \bar{w}_b)(t)|_{t=lT_c}$ be the chip-sampled discrete time equivalent FIR channel. The FIR channel $h_{m,b,a}(l)$ of order L_m includes the m-th user's asynchronism in the form of delay factors as well as transmit-receive filters, and frequency-selective multipath effects. Let $\eta_b(n) := (\eta \star \bar{w}_b)(t)|_{t=nT_c}$ denote sampled noise. The chip-sampled matched filter output of the b-th branch at the receiver is

$$x_b(n) = \sum_{m=0}^{M-1} \sum_{a=0}^{A-1} \sum_{l=0}^{L} h_{m,b,a}(l) u_{m,a}(n-l) + \eta_b(n). \quad (9)$$

We here focus on a cellular quasi-synchronous system in the *uplink*, where the mobile users attempt to synchronize with the base-station's pilot waveform, and have a coarse common timing reference. Asynchronism among users is thus limited to only a few chip intervals; the maximum asynchronism $\tau_{max,a}$ arises between the nearest and the farthest mobile users. With $\tau_{max,s}$ denoting maximum multipath spread, which is found using field measurements from the operational environment, the maximum channel order can be found as $L = \lceil (\tau_{max,s} + \tau_{max,a})/T_c \rceil$.

The *downlink* model (from the base station to the user of interest μ) is subsumed by the uplink model (9): indeed, setting $h_{m,b,a}(l) = h_{\mu,b,a}(l), \forall m \in [0, M-1]$, is a special case of (9) since the latter allows for distinct user channels. The downlink transmissions are synchronous with $\tau_{max,a} = 0$, and the maximum channel order L depends only on $\tau_{max,s}$ through $L = \lceil \tau_{max,s}/T_c \rceil$. In either uplink or downlink, the only channel knowledge assumed at the transmitter is L, and we always choose the block size $P \gg L$.

The received samples $x_b(n)$ are serial to parallel converted to form $P \times 1$ vectors:

$$\mathbf{x}_b(i) := [x_b(iP), x_b(iP+1), \ldots, x_b(iP+P-1)]^T.$$

Define the corresponding noise vector

$$\boldsymbol{\eta}_b(i) := [\eta_b(iP), \eta_b(iP+1), \ldots, \eta_b(iP+P-1)]^T;$$

and, let $\mathbf{H}_{m,b,a,0}$ be the $P \times P$ lower triangular Toeplitz matrix with first column $[h_{m,b,a}(0), \ldots, h_{m,b,a}(L), 0, \ldots, 0]^T$, and $\mathbf{H}_{m,b,a,1}$ be the $P \times P$ upper triangular Toeplitz matrix with first row $[0, \ldots, 0, h_{m,b,a}(L), \ldots, h_{m,b,a}(1)]$. The input-output block relationship of our system can be described in matrix-vector form as:

$$\begin{aligned} \mathbf{x}_b(i) = & \sum_{m=0}^{M-1} \sum_{a=0}^{A-1} \mathbf{H}_{m,b,a,0} \mathbf{u}_{m,a}(i) \\ & + \sum_{m=0}^{M-1} \sum_{a=0}^{A-1} \mathbf{H}_{m,b,a,1} \mathbf{u}_{m,a}(i-1) + \boldsymbol{\eta}_b(i), \end{aligned} \quad (10)$$

where $\mathbf{u}_{m,a}(i) := \mathbf{C}_m \tilde{\mathbf{s}}_{m,a}(i)$. Notice that the $\mathbf{u}_{m,a}(i-1)$ dependent term in (10) accounts for the so-called Inter-Block Interference (IBI).

IV. Digital CIBS-IRMA Design

We describe here our digital IRMA design that relies on block-spreading. The scheme is implemented by symbol-spreading followed by chip-interleaving as detailed in [12]. The resulting Chip-Interleaved Block-Spread (CIBS) based MUI-free transceivers are applicable to both $downlink$ and $uplink$ operations. Since PPM is a non-linear modulation, the receivers will operate in three stages: 1) a linear filtering stage to separate multiple users, and thus render the multiple-access channel to equivalent single-user ISI channel; 2) a linear filtering stage to eliminate channel effects by employing single-user channel equalizers; and 3) a symbol detection stage. Notice that in the second stage one can replace the linear equalizer by decision-feedback or maximum-likelihood nonlinear alternatives. However, targeting low-complexity, we will focus on three linear receive options.

To design the digital IRMA transmitters and receivers, we start by assigning to each user a distinct signature vector of length $P_{\tilde{c}} = N_f$ denoted by

$$\tilde{\mathbf{c}}_m = [\tilde{c}_m(0), \ldots, \tilde{c}_m(P_{\tilde{c}}-1)]^T, \quad (11)$$

with $\tilde{c}_m(n) \in [0, N_c - 1]$ and $\tilde{c}_m(n) \neq \tilde{c}_\mu(n), \forall n \in [0, P_{\tilde{c}} - 1]$. Let us define the user-specific spreading codes $\mathbf{c}_m = [c_m(0), \ldots, c_m(P_c - 1)]^T$ of length $P_c = N_c P_{\tilde{c}}$, and with $c_m(n)$ defined as in (7). It readily follows from (11) that these vectors are mutually orthogonal, i.e., $\mathbf{c}_m^{\mathcal{H}} \mathbf{c}_\mu = N_f \delta(m-\mu)$, $\forall m, \mu \in [0, M-1]$. Based on the orthogonal signature vectors $\{\mathbf{c}_m\}_{m=0}^{M-1}$, we next specify the block-spreading matrix $\mathbf{C}_m$, and the corresponding receiver matrix.

As mentioned earlier, the linear part of the receiver composes of two stages. The first stage employs a multiuser separating front-end, which is described by the matrix $\mathbf{G}_\mu$ for the μ-th user. Extracting the μ-th user from $\mathbf{x}_b(i)$ yields the MUI-free block:

$$\mathbf{y}_{\mu,b}(i) = \mathbf{G}_\mu^{\mathcal{H}} \mathbf{x}_b(i). \quad (12)$$

The MUI-free output $\mathbf{y}_\mu(i) := \left[\mathbf{y}_{\mu,0}^T(i), \ldots, \mathbf{y}_{\mu,A-1}^T(i)\right]^T$ can then be equalized by any single user equalizer; e.g., a linear equalizer $\mathbf{\Gamma}_\mu$ to yield symbol block estimates $\widehat{\tilde{\mathbf{s}}}_\mu(i)$:

$$\widehat{\tilde{\mathbf{s}}}_\mu(i) = \mathbf{\Gamma}_\mu \mathbf{y}_\mu(i). \quad (13)$$

Starting from the general block-spread transmission model, we will propose judiciously designed transceiver pairs $\{\mathbf{C}_m, \mathbf{G}_m\}_{m=0}^{M-1}$ that enable separation of superimposed multiuser signals deterministically, and *regardless of* multipath propagation through frequency-selective ISI channels of maximum order L.

Consider the $(K+L) \times K$ matrix $\mathbf{T}_{zp} := [\mathbf{I}_K, \mathbf{0}_{K \times L}]^T$, which we term zero-padding (ZP) matrix because upon pre-multiplication with an $K \times 1$ vector, it appends L zeros. Based on $\mathbf{T}_{zp}$, we select the $P \times K$ code matrices $\mathbf{C}_m$, and the corresponding $P \times (K+L)$ separating matrices $\mathbf{G}_m$ as:

$$\mathbf{C}_m = \mathbf{c}_m \otimes \mathbf{T}_{zp}, \quad \mathbf{G}_m = \mathbf{c}_m \otimes \mathbf{I}_{K+L}, \quad (14)$$

where using the Kronecker product definition we find that each user's code consists of $P = (K+L)P_c = N_1 + LP_c$ chips. The properties of Kronecker products ensure the mutual orthogonality among users:

$$\begin{aligned}\mathbf{C}_\mu^{\mathcal{H}}\mathbf{C}_m &= N_f\delta(\mu-m)\mathbf{I}_K,\\ \mathbf{G}_\mu^{\mathcal{H}}\mathbf{G}_m &= N_f\delta(\mu-m)\mathbf{I}_{K+L}.\end{aligned} \tag{15}$$

Recognizing that the last L rows of $\mathbf{C}_m$ are zero by design, while the non-zero elements of $\mathbf{H}_{m,b,a,1}$ only show up in its last L columns, we have

$$\mathbf{H}_{m,b,a,1}\mathbf{C}_m = \mathbf{0}_{P\times K}. \tag{16}$$

Let $\bar{\mathbf{H}}_{m,b,a,0}$ be the $(K+L)\times(K+L)$ lower triangular Toeplitz matrix with first column

$$[h_{m,b,a}(0),\ldots,h_{m,b,a}(L),0,\ldots,0]^T,$$

and $\bar{\mathbf{H}}_{m,b,a,1}$ be the $(K+L)\times(K+L)$ upper triangular Toeplitz matrix with first row

$$[0,\ldots,0,h_{m,b,a}(L),\ldots,h_{m,b,a}(1)].$$

We notice that the $P\times P$ matrix $\mathbf{H}_{m,b,a,0}$ in (10) can be split into smaller blocks as:

$$\mathbf{H}_{m,b,a,0} = \mathbf{I}_{P_c}\otimes\bar{\mathbf{H}}_{m,b,a,0} + \mathbf{J}_{P_c}\otimes\bar{\mathbf{H}}_{m,b,a,1}, \tag{17}$$

where $\mathbf{I}_{P_c}$ is the $P_c\times P_c$ identity matrix, and $\mathbf{J}_{P_c}$ is the $P_c\times P_c$ shifting matrix with first column $[0,1,0,\ldots,0]^T$. Making use of Kronecker product properties, we thus have

$$\mathbf{H}_{m,b,a,0}\mathbf{C}_m = \mathbf{G}_m\bar{\mathbf{H}}_{m,b,a,0}\mathbf{T}_{zp} = \mathbf{G}_m\check{\mathbf{H}}_{m,b,a}, \tag{18}$$

with $\check{\mathbf{H}}_{m,b,a}$ a tall Toeplitz matrix of dimension $(K+L)\times K$. Substituting (16) and (18) into (10), we have

$$\mathbf{x}_b(i) = \sum_{m=0}^{M-1}\mathbf{G}_m\sum_{a=0}^{A-1}\check{\mathbf{H}}_{m,b,a}\tilde{\mathbf{s}}_{m,a}(i) + \boldsymbol{\eta}_b(i). \tag{19}$$

Using (15) and (19), we can re-express (12) as:

$$\begin{aligned}\mathbf{y}_{\mu,b}(i) &= \mathbf{G}_\mu^{\mathcal{H}}\sum_{m=0}^{M-1}\mathbf{G}_m\sum_{a=0}^{A-1}\check{\mathbf{H}}_{m,b,a}\tilde{\mathbf{s}}_{m,a}(i) + \mathbf{G}_\mu^{\mathcal{H}}\boldsymbol{\eta}_b(i)\\ &= N_f\sum_{a=0}^{A-1}\check{\mathbf{H}}_{\mu,b,a}\tilde{\mathbf{s}}_{\mu,a}(i) + \tilde{\boldsymbol{\eta}}_b(i),\end{aligned} \tag{20}$$

with the substitution $\tilde{\boldsymbol{\eta}}_b(i) := \mathbf{G}_\mu^{\mathcal{H}}\boldsymbol{\eta}_b(i)$. Considering the $AK\times 1$ blocks $\tilde{\mathbf{s}}_\mu(i) := \left[\tilde{\mathbf{s}}_{\mu,0}^T(i),\ldots,\tilde{\mathbf{s}}_{\mu,A-1}^T(i)\right]^T$, we have

$$\mathbf{y}_\mu(i) = N_f\check{\mathbf{H}}_\mu\tilde{\mathbf{s}}_\mu(i) + \tilde{\boldsymbol{\eta}}(i), \tag{21}$$

where $\tilde{\boldsymbol{\eta}}(i)$ is an $A(K+L)\times 1$ vector, and $\check{\mathbf{H}}_\mu$ is an $A(K+L)\times AK$ matrix:

$$\check{\mathbf{H}}_\mu := \begin{bmatrix}\check{\mathbf{H}}_{\mu,0,0} & \check{\mathbf{H}}_{\mu,0,1} & \cdots & \check{\mathbf{H}}_{\mu,0,A-1}\\ \check{\mathbf{H}}_{\mu,1,0} & \check{\mathbf{H}}_{\mu,1,1} & \cdots & \check{\mathbf{H}}_{\mu,1,A-1}\\ \vdots & \vdots & \ddots & \vdots\\ \check{\mathbf{H}}_{\mu,A-1,0} & \check{\mathbf{H}}_{\mu,A-1,1} & \cdots & \check{\mathbf{H}}_{\mu,A-1,A-1}\end{bmatrix}.$$

Defining $\mathbf{x}(i) := [\mathbf{x}_0^T(i),\ldots,\mathbf{x}_{A-1}^T(i)]^T$, and $\mathbf{y}_\mu(i) := [\mathbf{y}_{\mu,0}^T(i),\ldots,\mathbf{y}_{\mu,A-1}^T(i)]^T$, and using (19) and (21), respectively, we find:

$$\begin{aligned}\mathbf{x}(i) &= \sum_{m=0}^{M-1}(\mathbf{I}_A\otimes\mathbf{G}_m)\check{\mathbf{H}}_m\tilde{\mathbf{s}}_m(i) + \boldsymbol{\eta}(i),\\ \mathbf{y}_\mu(i) &= (\mathbf{I}_A\otimes\mathbf{G}_\mu^{\mathcal{H}})\mathbf{x}(i).\end{aligned} \tag{22}$$

Eq. (22) confirms that the superimposed received signals from multiple users can be separated deterministically, regardless of the FIR multipath channels. This is due to the fact that the design in (14) preserves the code orthogonality among users even after *unknown* multipath propagation. As shown in [12], multipath channels with CIBS transmissions cause ISI within each symbol block, but they do not give rise to inter-chip interference (ICI) within the code vector $\mathbf{c}_m$; i.e., ICI is replaced by ISI, which in turn maintains the orthogonality among spreading codes at the receiver.

After MUI elimination, *any* single user equalizer can be applied to $\mathbf{y}_\mu(i)$ of (21) to remove the residual ISI. Here we consider only linear equalizers. Depending on how $\boldsymbol{\Gamma}_\mu$ is selected, we obtain the following three linear receivers:

- *MF receiver:*

$$\boldsymbol{\Gamma}_\mu^{MF} := \check{\mathbf{H}}_\mu^{\mathcal{H}}/N_f, \tag{23}$$

- *ZF receiver:*

$$\boldsymbol{\Gamma}_\mu^{ZF} := \left(\check{\mathbf{H}}_\mu^{\mathcal{H}}\check{\mathbf{H}}_\mu\right)^{-1}\check{\mathbf{H}}_\mu^{\mathcal{H}}/N_f, \tag{24}$$

- *MMSE receiver:*

$$\boldsymbol{\Gamma}_\mu^{MMSE} := N_f\mathbf{R}_\mu\check{\mathbf{H}}_\mu^{\mathcal{H}}\left[\mathbf{R}_{\bar{\eta}} + N_f^2\check{\mathbf{H}}_\mu\mathbf{R}_\mu\check{\mathbf{H}}_\mu^{\mathcal{H}}\right]^{-1}, \tag{25}$$

where $\mathbf{R}_\mu := \mathbf{E}\{\tilde{\mathbf{s}}_\mu(i)\tilde{\mathbf{s}}_\mu^{\mathcal{H}}(i)\}$, and $\mathbf{R}_{\bar{\eta}} := \mathbf{E}\{\tilde{\boldsymbol{\eta}}(\mathbf{i})\tilde{\boldsymbol{\eta}}^{\mathcal{H}}(\mathbf{i})\}$.

Symbol detection is then performed based on the soft estimates $\widehat{\tilde{\mathbf{s}}}_\mu(i)$. Defining the μ-th user's $K\times 1$ symbol block estimate $\hat{\mathbf{s}}_\mu := [\hat{s}_\mu(iK),\hat{s}_\mu(iK+1),\ldots,\hat{s}_\mu(iK+K-1)]^T$, decisions can be made according to:

$$\hat{s}_\mu(iK+k) = a_0 : \widehat{\tilde{s}}_{\mu,a_0}(iK+k) = \max_a\{\widehat{\tilde{s}}_{\mu,a}(iK+k)\},$$

where $a, a_0\in[0,A-1]$ and $k\in[0,K-1]$.

V. Simulation Results

To illustrate the performance of the proposed IRMA scheme, we simulate both the novel MUI-free CIBS-IRMA, and the MUD-IRMA in [4]. Since the latter one only applies to downlink, we simulate downlink operation for both transceivers. The PPM parameters are as follows: alphabet size $A=2$, which corresponds to a binary modulation, with every symbol transmitted repeatedly over $N_f=3$ frames, each frame composed of $N_c=8$ chips, allowing a maximum user number $M=8$, and the block size $K=2$. As in [9], we have chosen the frame duration $T_f = 100ns$, which is also the maximum delay spread.

In our simulations, two channel models are employed. In the first one, the channel is modeled with 400 paths equally

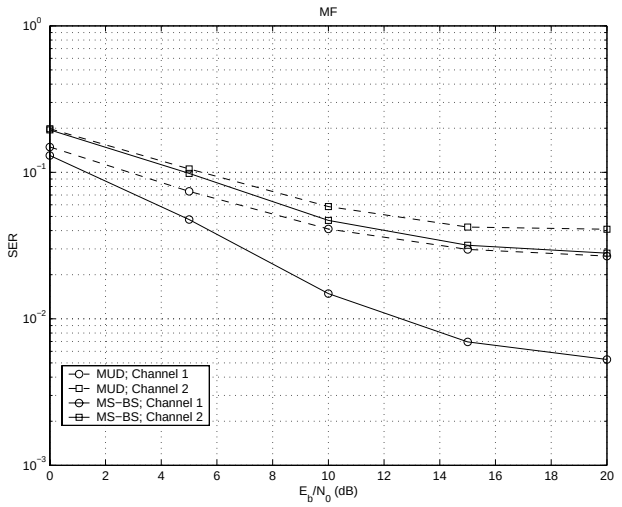

Fig. 2. SER vs. E_b/N_0 for MF receiver for binary symbols with $N_f = 3$, $N_c = 8$, and $K = 2$.

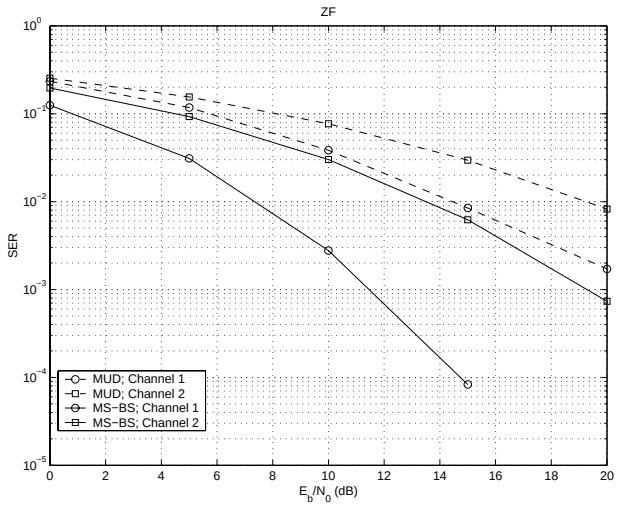

Fig. 3. SER vs. E_b/N_0 for ZF receiver for binary symbols with $N_f = 3$, $N_c = 8$, and $K = 2$.

spaced in time within the maximum delay spread. The amplitude of each path is modeled as a Gaussian variable, and is linearly weighted decreasing to zero at the maximum delay spread. The second channel model is generated according to [5, 3], where rays arrive in several clusters within an observation window. The cluster arrival times are modeled as a Poisson process with cluster arrival rate Λ. Rays within each cluster also arrive according to a Poisson process with ray arrival rate λ. The amplitude of each arriving ray is a Rayleigh distributed random variable with exponentially decaying mean square value. Parameters of this channel model are chosen as: $\Gamma = 33ns$, $\gamma = 5ns$, $1/\Lambda = 2ns$, and $1/\lambda = 0.5ns$. We select the pulse shaper to be the second derivative of the Gaussian function $w(t) = \sqrt{\tau^3/3}(2/\pi)^{1/4}\exp(-t^2/\tau^2)$, which has been normalized to have unit energy. The parameter τ is chosen to be $0.1225ns$ to obtain a pulse width of $0.7ns$.

Figures 2 through 4 depict the Symbol Error Rate (SER) for the three receivers based on the two digital IRMA schemes. For both channel models, the MF receiver performs poorly, and exhibits a SER floor as the SNR goes to infinity (see Fig. 2). We also notice that the CIBS-MF receivers lead to a lower SER floor for both channels. In all cases, the MMSE receiver shows the best performance, and the CIBS receivers consistently outperform their MUD counterparts.

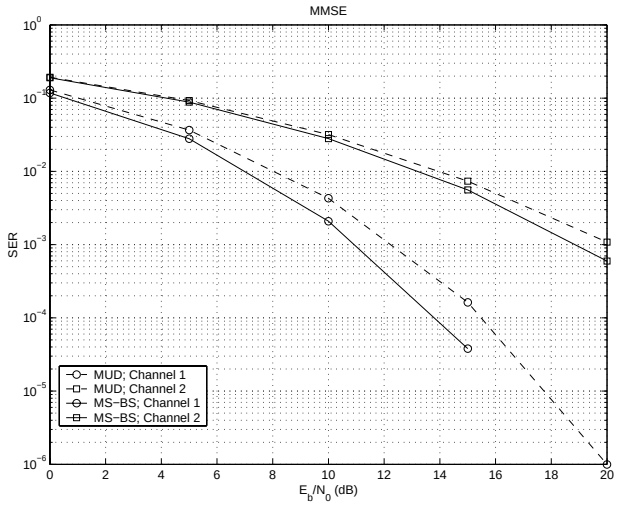

Fig. 4. SER vs. E_b/N_0 for MMSE receiver for binary symbols with $N_f = 3$, $N_c = 8$, and $K = 2$.

REFERENCES

[1] S. S. Kolenchery, K. Townsend, J. A. Freebersyser, and G. Bilbro, "Performance of Local Power Control in Peer-to-peer Impulse Radio Networks with Bursty Traffic," in *Proc. of Globecom.*, Phoenix, AZ, USA, pp. 910-916, Nov. 1997.

[2] S. S. Kolenchery, K. Townsend and J. A. Freebersyser, "A Novel Impulse Radio Network for Tactical Wireless Communications," in *Proc. of the Milcom Conf.*, Bedford, MA, USA, pp. 59-65, Oct. 1998.

[3] H. Lee, B. Han, Y. Shin, and S. Im, "Multipath characteristics of impulse radio channels," in *Vehicular Technology Conference Proceedings*, Tokyo, Spring 2000, pp. 2487 -2491.

[4] C. J. Le Martret and G. B. Giannakis, "All-digital PPM Impulse Radio for Multiple-Access through Frequency-Selective Multipath," in *Proc. of Sensor Array and Multichannel Signal Processing Workshop*, Boston, March 2000, pp. 22-26.

[5] A. A. M. Saleh and R. A. Valenzuela, "A Statistical Model for Indoor Multipath Propagation," *IEEE Journal on Selected Areas in Communications*, Vol. JSAC-5, no. 2, pp. 128-137, Feb. 1987.

[6] R. A. Scholtz, "Multiple Access with Time-hopping Impulse Radio," in *Proc. of the Milcom Conf.*, Boston, MA, USA, Oct. 1993, pp. 447-450.

[7] Z. Wang and G. B. Giannakis, "Wireless Multicarrier Communications: Where Fourier meets Shannon," *IEEE Signal Processing Magazine*, Vol. 17, No. 3, pp. 29-48, May 2000.

[8] M. Z. Win, R. A. Scholtz, "Impulse Radio: How It Works," *IEEE Communications Letters*, Vol. 2, No. 2, pp. 36-38, Feb. 1998.

[9] M. Z. Win, X. Qiu, R. A. Scholtz, and V. O. K. Li, "ATM-based TH-SSMA Network for Multimedia PCS," *IEEE Journal on Selected Areas in Communications*, Vol. 17, No. 5, pp. 824-836, May 1999.

[10] M. Z. Win, R. A. Scholtz, "Ultra-Wide Bandwidth Time-Hopping Spread-Spectrum Impulse Radio for Wireless Multiple-Access Communications," *IEEE Transactions on Communications*, Vol. 48, No. 4, pp. 679-691, April 2000.

[11] P. II. Withington and L. W. Fullerton, "An Impulse Radio Communications System," *Proc. of the Intl. Conf. on Ultra-Wide Band, Short-Pulse Electromagnetics*, Brooklyn, NY, USA, Oct. 1992, pp.113-120.

[12] S. Zhou and G. B. Giannakis, and C. Le Martret, "Chip-Interleaved Block-Spread Code Division Multiple Access," *IEEE Trans. on Communications*, Feb. 2002 (to appear).